Experimental Comparison of Two Degrees-of-Freedom Vortex-Induced Vibration on High and Low Aspect Ratio Cylinders with Small Mass Ratio

Rodolfo T. Gonçalves[1]
e-mail: rodolfo_tg@tpn.usp.br

Guilherme F. Rosetti
e-mail: guilherme.feitosa@tpn.usp.br

André L. C. Fujarra
e-mail: afujarra@usp.br

TPN – Numerical Offshore Tank,
Department of Naval Architecture
and Ocean Engineering,
Escola Politécnica – University of São Paulo,
Avenue Professor Mello Moraes, 2231,
Cidade Universitária,
São Paulo, SP, 05508-900, Brazil

Guilherme R. Franzini
e-mail: gfranzini@usp.br

César M. Freire
e-mail: cesar.freire@usp.br

Julio R. Meneghini
e-mail: jmeneg@usp.br

NDF – Fluid & Dynamics Research Group,
Department of Mechanical Engineering,
Escola Politécnica – University of São Paulo,
São Paulo, SP, 05508-900, Brazil

Vortex-induced motion (VIM) is a specific way for naming the vortex-induced vibration (VIV) acting on floating units. The VIM phenomenon can occur in monocolumn production, storage and offloading system (MPSO) and spar platforms, structures presenting aspect ratio lower than 4 and unity mass ratio, i.e., structural mass equal to the displaced fluid mass. These platforms can experience motion amplitudes of approximately their characteristic diameters, and therefore, the fatigue life of mooring lines and risers can be greatly affected. Two degrees-of-freedom VIV model tests based on cylinders with low aspect ratio and small mass ratio have been carried out at the recirculating water channel facility available at NDF-EPUSP in order to better understand this hydro-elastic phenomenon. The tests have considered three circular cylinders of mass ratio equal to one and different aspect ratios, respectively L/D = 1.0, 1.7, and 2.0, as well as a fourth cylinder of mass ratio equal to 2.62 and aspect ratio of 2.0. The Reynolds number covered the range from 10 000 to 50 000, corresponding to reduced velocities from 1 to approximately 12. The results of amplitude and frequency in the transverse and in-line directions were analyzed by means of the Hilbert-Huang transform method (HHT) and then compared to those obtained from works found in the literature. The comparisons have shown similar maxima amplitudes for all aspect ratios and small mass ratio, featuring a decrease as the aspect ratio decreases. Moreover, some changes in the Strouhal number have been indirectly observed as a consequence of the decrease in the aspect ratio. In conclusion, it is shown that comparing results of small-scale platforms with those from bare cylinders, all of them presenting low aspect ratio and small mass ratio, the laboratory experiments may well be used in practical investigation, including those concerning the VIM phenomenon acting on platforms. [DOI: 10.1115/1.4006755]

Keywords: VIV, VIM, low aspect ratio, small mass ratio, two degrees-of-freedom, model tests

1 Introduction

From the earliest evidence in spar platforms, the VIM phenomenon has shown close similarity to the phenomenological aspects of VIV on remarkably slender structures, such as risers.

In fact, the small-scale experiments on a truss spar platform performed by van Dijk et al. [1] already showed that, despite the strong susceptibility to geometric aspects of the hull, the VIM phenomenon clearly presents both the self-excitation and the self-controlled characteristics, in general terms, similar to the VIV on risers. Moreover, despite focused on mitigating the effects of VIM on such a type of platform by adding strakes, those authors also showed that, without suppressors, the maximum response amplitude occurs in a range of reduced velocities between 5 and 9, making explicit mention to eight-shaped trajectories, in a quite evident coupling between the in-line and transverse motions. Additionally, experiments by Finn et al. [2] established a direct relationship between hull geometry and VIM response, highlighting the correlation between towing tests and those performed at water channels. According to those results, a formal procedure for testing VIM on spar-type platforms was presented in Irani and Finn [3], including concerns about the right consideration of the restoring system in small-scale tests. By focusing on operational conditions and concurrently aware of the VIM susceptibility to other hydrodynamic mechanisms, Finnigan et al. [4] started experiments considering VIM and free surface waves simultaneously. In general, those authors found that the waves have a mitigating effect on the VIM phenomenon by reducing its response amplitude; however, without an explanation for such interaction. Recently, Roddier et al. [5] conducted a study to verify the influence of the Reynolds number on the VIM phenomenon, according to which the tests carried out at lower values of Reynolds were found to be conservative, presenting maximum amplitudes of motion greater than those observed in the full-scale tests. Unlike all previous works, Wang et al. [6] focused on testing models without appendages (bare cylinders with low aspect ratio, L/D), being one of the earliest initiatives in establishing a direct relationship between VIM and VIV; therefore, deriving its importance for the comparisons presented later in this work.

Even more surprisingly, as in results from spar platforms, VIM phenomenon occurred on platforms with lower aspect ratios, $L/D < 0.5$, called monocolumn platforms as presented and discussed in Gonçalves et al. [7]. According to Gonçalves et al. [7], in 2005 a partnership between the research group from USP – University of São Paulo and Petrobras started a pioneer and intensive experimental research on VIM of monocolumn platforms. Cueva et al. [8], Fujarra et al. [9], and Gonçalves et al. [10] established experimental procedures for VIM tests on monocolumns, besides proposing a more accurate technique for analyzing

[1]Corresponding author.

Contributed by the Design Engineering Division of ASME for publication in the Journal of Vibration and Acoustics. Manuscript received March 4, 2011; final manuscript received December 13, 2011; published online October 29, 2012. Assoc. Editor: Massimo Ruzzene.

the outcomes. Moreover, even for very low aspect ratios, the research showed that VIM on monocolumns also presents large amplitudes of transversal motion above reduced velocities of 4. Later, in Gonçalves et al. [11], many mitigation aspects were investigated, such as the presence of appendages on the hull (stairs, fairleads, etc.), the coexistence of waves on the free surface and the damping promoted by risers, umbilicals and mooring lines. Surely, the most important aspect for the VIM mitigation was the aspect ratio, investigated by means of the draft variation of the small-scale monocolumns. In fact, in Gonçalves et al. [12], the USP research group carried out a comparison work between results from both VIM on monocolumn platforms and VIV on smooth cylinders, by using as a benchmark parameter the aspect ratio L/D. As a result, the authors confirmed the similarity between VIM and VIV phenomena, simply affected by the consequences of modifying the shedding pattern of vortices downstream of a cylinder with a given aspect ratio.

In order to increase the understanding concerning the similarity between VIM and VIV phenomena, in the present work new experiments were carried out with rigid cylinders of low aspect ratio ($1.0 < L/D < 2.0$) and small mass ratios, $m^* < 3.00$ in a recirculating water channel, by using two distinct elastic supports (a cantilevered beam and a pivoted beam). The comparison between results from different apparatuses has ensured the reliability for subsequent comparison with similar results reported in the literature.

For this last part of the comparison, some results of VIV with two degrees-of-freedom were used, among them: Pesce and Fujarra [13] by means of a cantilevered flexible cylinder with $m^* = 2.36$ and $L/D = 94.50$; Jauvtis and Williamson [14] through a rigid cylinder elastically supported with $m^* = 2.62$ and $L/D = 10.00$; Sanchis et al. [15] by means of a spring mounted cylinder with $m^* = 1.04$ and $L/D = 6.00$; Stappenbelt and Lalji [16] and Blevins and Coughran [17] both based on elastically mounted rigid cylinders, but the former one with $m^* = 2.36$ and $L/D = 8.00$ and the latter with $m^* = 1.00$ or 2.36 and $L/D = 17.80$; as well as Freire and Meneghini [18] considering a rigid cylinder mounted in a pivoted beam with $m^* = 2.80$ and $L/D = 21.88$.

Furthermore, and closer to the tangible behavior observed for VIM on offshore structures, the results obtained in the present work were also compared to those from the mentioned experiments performed by Wang et al. [6] in floating rigid cylinders with $L/D = 2.40$ and by Gonçalves et al. [11] in small-scale platforms with $L/D = 0.39$. Since those are floating cylinders, in both cases the mass ratio was equal to 1.

Importantly, the results with two degrees-of-freedom are fairly recent and thus, besides those cited references, many other works deserve to be mentioned, since they have been a source of phenomenological aspects for the discussion herein presented. Among them, Fujarra et al. [19], Jauvtis and Williamson [14,20]; Flemming and Williamson [21]; Dahl et al. [22]; Leong and Wei [23], and Marzouk [24] should be mentioned.

2 Experimental Setup

The experiments were performed making use of two different experimental apparatuses (see an example of the apparatuses in Fig. 1). The first set of tests was carried out by means of a rigid cylinder elastically supported by a cantilevered beam and the second one by means of a pivoted rigid pendulum. Details about the first setup can be found in Gonçalves et al. [12] and Franzini et al. [25], whereas the second is described in detail in Freire et al. [26] and Freire and Meneghini [18].

Both tests were performed at the recirculating water channel facility available at NDF – Fluid and Dynamics Research Group at the University of São Paulo, Brazil. This facility has a $0.70 \times 0.70 \times 7.50$ m test section, presenting a very low level of turbulence (less than 1%) and operating at well-controlled free-stream velocity up to 0.70 m/s, although the maximum velocity reached in this work was close to 0.40 m/s. Further details concerning the recirculating water channel can be found in Assi et al. [27].

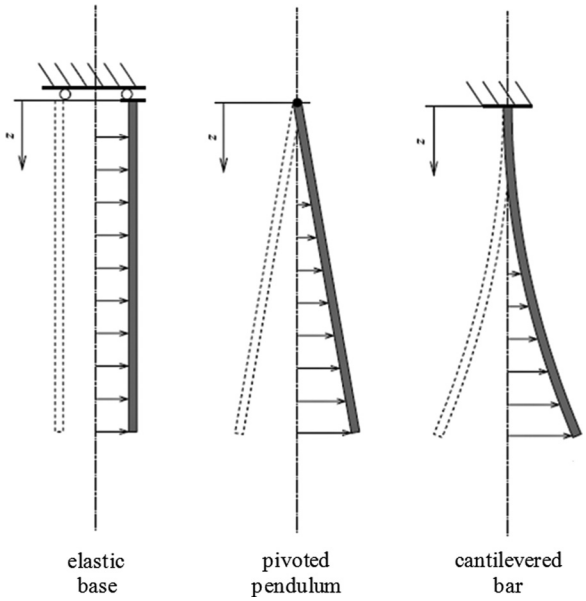

Fig. 1 Example of different apparatuses for VIV study. Source: Flemming & Williamson [21].

In terms of the acquiring procedure, all the time histories of movement for both arrangements were acquired considering at least 180 s. The flow velocities were achieved by steps, between which 120 s were taken into account in order to avoid transient effects due to the flow acceleration, and therefore assuring enough time for stabilizing the flow velocities. Time series of displacement were obtained by using two laser position sensors.

2.1 The Elastic Support Based on a Cantilevered Beam. A rigid cylinder with 125 mm in diameter was attached to the end of a cantilevered beam, free to oscillate in two degrees-of-freedom (in-line and transverse directions); see direction definition in Fig. 2. This apparatus presents the same natural frequency in both directions and its structural damping coefficient is very low, determined by free-decay tests conducted in air and equal to

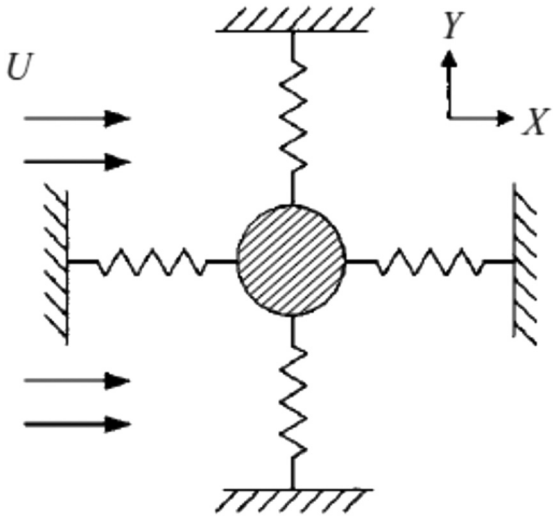

Fig. 2 Definitions of two degrees-of-freedom experiments, where X is the flow, U, direction (in-line) and Y is the transverse direction (cross-flow). Source: Jauvtis & Williamson [14].

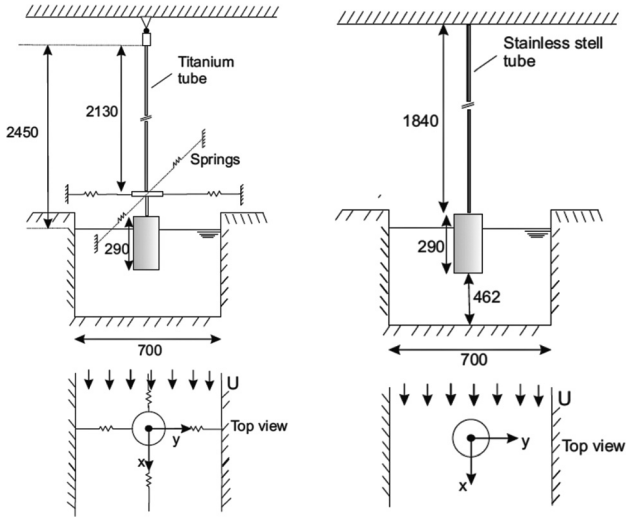

Fig. 3 Main characteristics of the experimental apparatus, on the left, rigid cylinder mounted in a pendulum, and on the right, rigid cylinder mounted in a cantilevered beam

approximately $\zeta_s = 0.1\%$. The stiffness of the system is defined by the length of the cantilevered beam, selected in order to adjust the reduced velocity range to the water channel capability, see Fig. 3.

Two values of aspect ratio were tested by changing the water level in the channel, $L/D = 1.5$ and 2.0, both combined with two different values of the mass ratio parameter, $m^* = 1.00$ and 2.62.

2.2 The Elastic Support Based on a Pivoted Pendulum. The same rigid cylinder was also mounted in a pivoted rigid pendulum support with two degrees-of-freedom. This apparatus presents the same natural frequency in both directions, also with low structural damping around the Cardan-joint at the top end of the pendulum, see Fig. 3.

In this case, for all the experiments, the mass ratio was kept constant and equal to unity by adding small lumped masses to the model. Furthermore, three aspect ratios were considered in these experiments, $L/D = 1.45, 1.70,$ and 2.00, again obtained by changing the water level of the channel.

3 Means of Comparison

All the transverse and in-line displacements were compared at the free end of the elastically supported cylinder. In order to compare the results from different structural apparatuses, a modal form factor γ_n is appropriate, as presented, for example, in Blevins [28].

Ruling the time dependence out, one can present the transverse amplitude displacement along the structural span as

$$y_n(z) = A_n \bar{\varphi}_n(z) \tag{1}$$

where z is the spanwise coordinate, measured downward, and $\bar{\varphi}_n(z) = \varphi_n(z)/\varphi_n^{\max}$ is the nth normalized eigenmode. In this case, A_n is the corresponding eigenmode amplitude that, from standard equations in the theory of strength of materials, reads

$$A_n = \frac{\varepsilon(z)}{h\bar{\varphi}_n''(z)} \tag{2}$$

where $\varepsilon(z)$ is the flexural strain in station z, $h = d/2$ is the structural half diameter, and $\bar{\varphi}_n''(z)$ is the curvature of the nth eigenmode. From the Euler beam theory, neglecting tension due to immersed weight, the following eigenmode shape is valid:

$$\varphi_n(z) = \sigma_n\left[\sin\left(\frac{\alpha_n z}{L}\right) - \sinh\left(\frac{\alpha_n z}{L}\right)\right] + \cos\left(\frac{\alpha_n z}{L}\right) - \cosh\left(\frac{\alpha_n z}{L}\right) \tag{3}$$

$$\sigma_n = \frac{\sin(\alpha_n) - \sinh(\alpha_n)}{\cos(\alpha_n) + \cosh(\alpha_n)} \tag{4}$$

$$\cos(\alpha_n)\cosh(\alpha_n) + 1 = 0 \tag{5}$$

As is well known, the nondimensional transverse displacement with respect to the incident flow can be made nondimensional with respect to the cylinder diameter D,

$$Y_n^* = \frac{Y_n}{\gamma_n D} \tag{6}$$

normalized by a modal form factor γ_n defined by

$$\gamma_n = \left\{\frac{\int_0^L \varphi^2(z)dz}{\int_0^L \varphi^4(z)dz}\right\}^{1/2} \tag{7}$$

which, in the present case, takes the value $\gamma_{n=1} = \gamma = 1.305$ for the first flexural mode of the cantilevered beam and $\gamma = 1.291$ for the pivoted pendulum, since, in this case, $\varphi(z) = z/L$. For the sake of conciseness, from now on, only the nomenclature γ will be adopted.

Table 1 Results compared in the present work

Work	m*	L/D	Re	γ	Apparatus
Pesce and Fujarra [13]	2.36	94.50	6,000–40,000	1.305	Vertical flexible cylinder (cantilever beam)
Jauvtis and Williamson [14]	2.62	10.00	1,000–15,000	1.000	Vertical rigid cylinder (elastic support)
Stappenbelt and Lalji [16]	2.36	8.00	12,600–84,000	1.000	Vertical rigid cylinder (elastic support)
Sanchis et al. [15]	1.04	6.00	13,000–18,600	1.000	Vertical rigid cylinder (elastic support)
Wang et al. [6]	1.00	2.40	18,400–42,000	1.000	Vertical floating cylinder
Blevins and Coughran [17]	1.00	17.8	2,000–11,000	1.000	Vertical rigid cylinder (elastic support)
	2.56				
Gonçalves et al. [12]	1.00	0.39	20,000–1,000,000	1.000	Vertical floating cylinder
Freire and Meneghini [18]	2.80	21.88	1,000–7,000	1.291	Vertical rigid cylinder (pivoted pendulum)
Present work	1.00	2.00	10,000–50,000	1.291	Vertical rigid cylinder (pivoted pendulum)
		1.70			
		1.45			
Present work	1.00	2.00	10,000–50,000	1.305	Vertical rigid cylinder (cantilever beam)
	1.00	1.50			
	2.62	2.00			

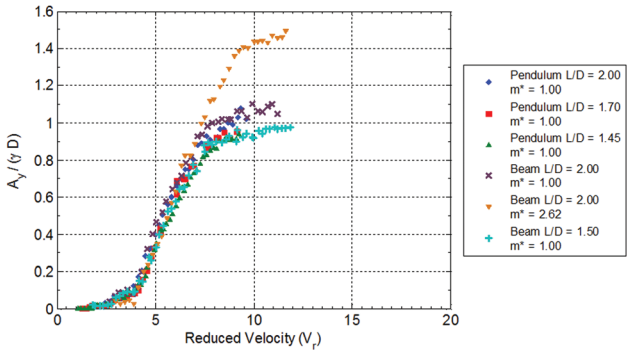

Fig. 4 Nondimensional results for motions in the transverse direction of two degrees-of-freedom VIV on cylinders with low aspect ratio ($L/D \leq 2.0$) and small mass ratio ($m^* \leq 3.0$)

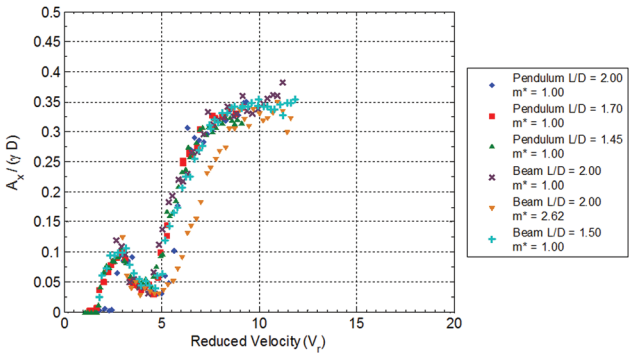

Fig. 5 Nondimensional results for motions in the in-line direction of two degrees-of-freedom VIV on cylinders with low aspect ratio ($L/D \leq 2.0$) and small mass ratio ($m^* \leq 3.0$)

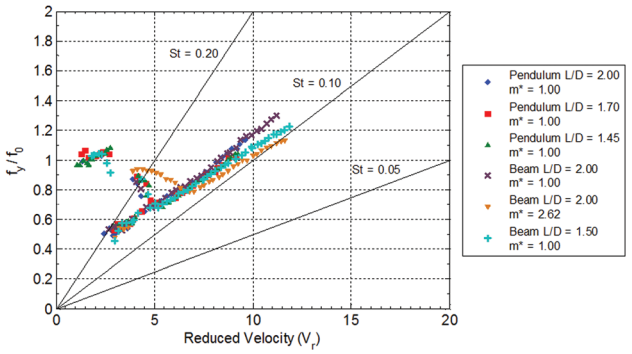

Fig. 6 Nondimensional results of transverse oscillation frequency and natural transverse frequency in still water for two degrees-of-freedom VIV on cylinders with low aspect ratio ($L/D \leq 2.0$) and small mass ratio ($m^* \leq 3.0$)

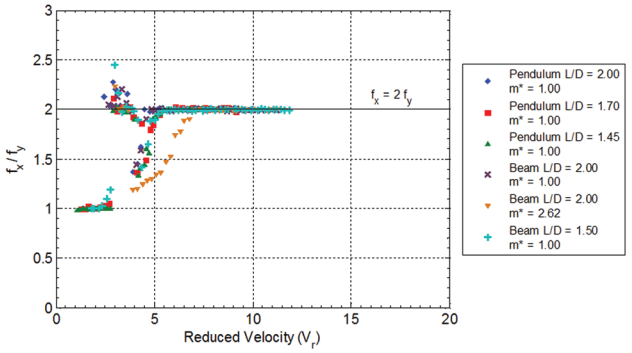

Fig. 7 Nondimensional results of in-line oscillation frequency and transverse one for two degrees-of-freedom VIV on cylinders with low aspect ratio ($L/D \leq 2.0$) and small mass ratio ($m^* \leq 3.0$)

In terms of signal processing, the experimental results of VIV on the low aspect ratio cylinders were analyzed by means of the Hilbert-Huang transform method (HHT). Details about the procedure to define the characteristic amplitudes and frequencies by using HHT on VIV signals can be found in Gonçalves et al. [29].

The HHT was developed in Huang et al. [30] as an alternative to deal with nonstationary signals that arise from nonlinear systems. By performing this analysis, the amplitude and the instantaneous frequency can be presented as functions of time in a three-dimensional graph, the so-called *Hilbert-Huang spectrum*, $H(\omega, t)$. Consequently, the HHT is extremely indicated for amplitude and frequency modulation, characteristics frequently found in VIV signals. Moreover, the distribution of energy is more accurately performed as energy can be locally concentrated in a range of frequencies and not all along. As the VIV signals can be rather nonstationary, it is also difficult to define the amplitude of the signal by the usual analysis. This is another issue that HHT can resolve as local amplitude is obtained regardless of the nonstationary behavior.

As a final step in this means of analysis, the nondimensional amplitude was defined by taking the mean of the 10% largest amplitudes as obtained in the HHT, both for motion in the transverse and in-line directions. It is important to highlight that in the HHT the amplitudes of displacement are a function of time, then the mean of the 10% largest amplitudes is proportional to the length of data, and consequently, to the sampling frequency, which implies an improvement of the statistic characteristics.

4 Results

The results presented in this section are twofold. Firstly, the experimental results of the low aspect ratio cylinders supported on a cantilevered beam and pivoted pendulum are presented. Then, these results are compared with those from the literature for similar tests in terms of aspect ratio and mass ratio.

Table 1 summarizes all the important parameters for the comparisons and conclusions presented herein.

4.1 Cylinders Elastically Supported on a Cantilevered Beam and Pivoted Pendulum Results. Figure 4 presents nondimensional transverse amplitudes for the experiments with the cantilevered beam and pivoted pendulum apparatus. Firstly, one can realize that indeed the modal form factor is essential for establishing a common base for comparison of results from different experimental apparatuses. Specifically, we refer to the comparison between pendulum and cantilevered beam results for $m^* = 1.00$, respectively, featured by $L/D = 2.00$ and $L/D = 1.45 - 1.50$. As expected, one notices that the amplitudes and trends are very similar since the mass and aspect ratios are common.

On the one hand, by comparing the results for different aspect ratios and mass ratio equal to unity, one can perceive two aspects. Firstly, that higher aspect ratios tend to present higher amplitudes, e.g., $A_y/(\gamma D) \cong 1.10$ for $L/D = 2.00$ and $A_y/(\gamma D) \cong 1.00$ for $L/D = 1.45 - 1.50$. It is expected that the free end of the cylinder disturbs the flow in a three-dimensional manner in such a way that it may explain the differences for the cylinders with low aspect ratios. Also, there is a more delicate aspect related to a shift in the curves to the right, which can be possibly related to the change in the Strouhal number for different aspect ratios.

On the other hand, looking at different mass ratios, there is an unexpected increase in amplitudes for the larger mass ratio, e.g., $A_y/(\gamma D) \cong 1.50$ for $m^* = 2.62$ and compared to $A_y/(\gamma D) \cong 1.10$ for $m^* = 1.00$.

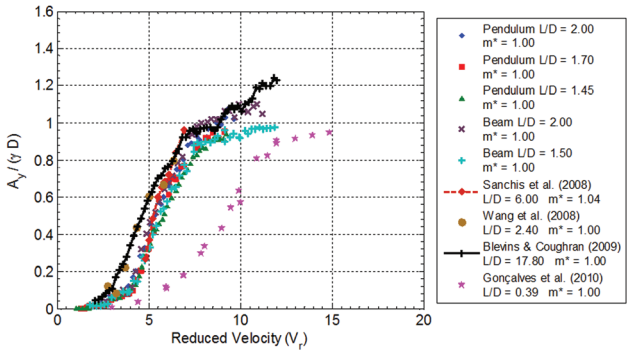

Fig. 8 Comparison between nondimensional results for motions in the transverse direction of two degrees-of-freedom VIV on cylinders with mass ratio approximately equal to the unity ($m^* = 1.00$)

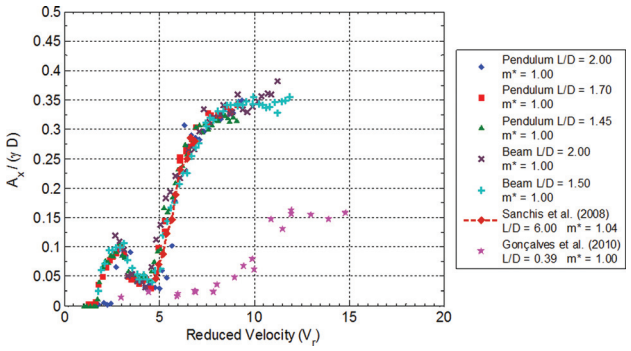

Fig. 9 Comparison between nondimensional results for motions in the in-line direction of two degrees-of-freedom VIV on cylinders with mass ratio approximately equal to the unity ($m^* = 1.00$)

As a general trend observed through all results, one cannot identify a well-defined lower branch, perhaps because the experiments conducted in this work could not reach higher values of reduced velocity.

Figure 5 presents the nondimensional in-line amplitudes for the same experiments. Regarding the aspect ratio effect, no great difference is observed between the results from the different cases, whereas for different mass ratios, there is a distinct behavior for the high-mass ratio case, with slightly lower amplitudes and a shift to the right as a probable result of the later synchronization observed in Fig. 7 below.

A lower peak of amplitude in $V_r \cong 2.50$ can also be noticed by inspecting Fig. 7, which should be due to the "in-line resonance," as previously mentioned by Blevins and Coughran [17]. However, higher amplitudes became evident at the same range of reduced velocity; as a result of the coupling between transverse and in-line motions.

Figure 6 presents the frequency response in the transverse direction, normalized by the natural frequency in still water. Similarly, the frequency response for the in-line direction is presented in Fig. 7. As normally adopted by the literature, the comparison between in-line and transverse frequencies are made by normalizing both through the transversal natural frequency in still water.

According to those figures, below $V_r = 3.00$ both transverse and in-line frequencies are quite similar to the transverse natural frequency, being predominant the in-line motion as a result of the resonance in this degree-of-freedom. For $V_r \geq 3.00$, there is evident coupling between transverse and in-line motions, featured by the in-line frequency twice the transverse one. In Fig. 6, probably resulting from the effect of the small mass ratio, the range of

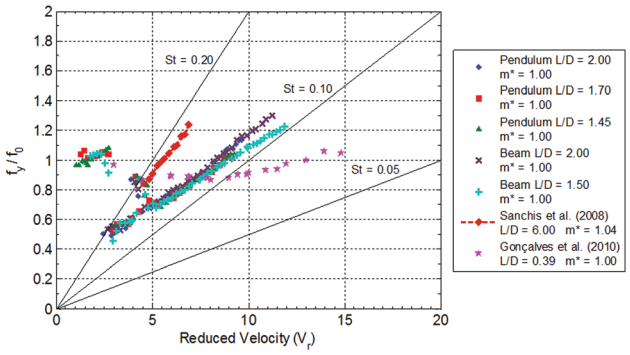

Fig. 10 Comparison between nondimensional results of transverse oscillation frequency and transverse natural frequency in still water for two degrees-of-freedom VIV on cylinders with mass ratio approximately equal to the unity ($m^* = 1.00$)

reduced velocities corresponding to the increase of response amplitudes, $V_r > 5.00$, is not observed as the classical definition for the synchronization region, where $f_y/f_o \approx 1$.

For the case of $m^* = 2.62$, both transverse and in-line frequencies synchronized later than for $m^* = 1.00$, consistent with the amplitudes results.

4.2 Results Compared to Those From the Literature. Figure 8 compares the results herein presented for $m^* = 1.00$ with those found in the literature, namely results from Wang et al. [6] testing a small-scale spar platform and from Gonçalves et al. [11] testing a small-scale monocolumn platform, as well as from Sanchis et al. [15] and Blevins and Coughran [17] both based on cylinders elastically supported with two degrees-of-freedom.

In general, it can be observed that the higher peak amplitudes correspond to the cases of higher aspect ratio, possibly as a result of a better correlation spanwise in the shedding vortices. Also, as mentioned before, it is possibly related to the changes on the Strouhal number for lower aspect ratios, shifting the curves to the right. This effect may easily be confirmed by comparing the lowest to the highest aspect ratio. For $L/D = 17.8$ from Blevins and Coughran [17], there is an early synchronization as that found for "infinite" cylinder submitted to VIV phenomenon. On the other hand, for $L/D = 0.39$ by Gonçalves et al. [11], the synchronization occurs later, possibly due to the smaller Strouhal number involved, similar to those of the VIM phenomenon on platforms.

Furthermore, owing to the stability of the flow, it is equally interesting and important to notice that, even though the results are from different experimental apparatuses, namely bare cylinders and small-scale models of platforms with appendages, the curves are quite similar in trend and also in nondimensional values. Thus, it is definitely confirmed that laboratory experiments may be used in a practical investigation, even for the VIM phenomenon. In fact, VIV and VIM present the same phenomenological aspects and close comparisons between them can be performed.

Figure 9 compares the in-line amplitudes for the same $m^* = 1.00$ case. The literature results are those presented in Gonçalves et al. [11] for $L/D = 0.39$ and in Sanchis et al. [15] for $L/D = 6.00$. Consistently with the transverse results, the in-line amplitudes show a later synchronization and lower amplitudes for the lower aspect ratio cases, which means $A_x/(\gamma D) \cong 0.15$ for $L/D = 0.39$ compared to $A_x/(\gamma D) \cong 0.35$ for the other aspect ratios.

Figure 10 presents frequencies of transverse oscillations normalized by the transverse natural frequency in still water. It is well know that the angular coefficient of the line out of the synchronization region is related to the Strouhal number and, as can be noticed, for different aspect ratios, this coefficient is quite

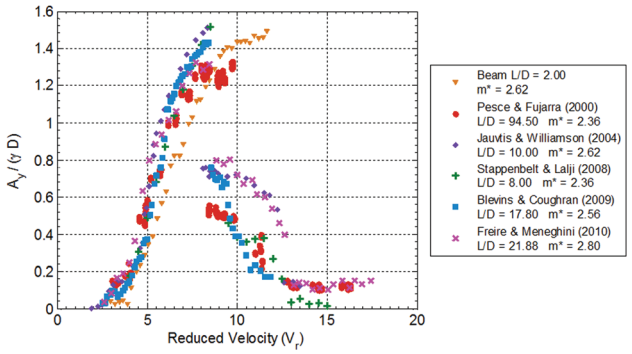

Fig. 11 Comparison between nondimensional results for motions in the transverse direction of two degrees-of-freedom VIV on cylinders with small mass ratio ($m^* \leq 3.0$)

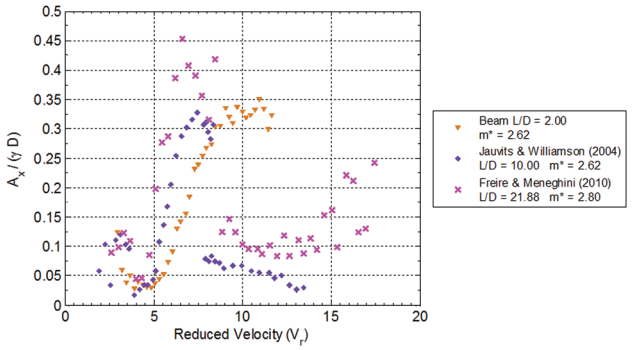

Fig. 12 Comparison between nondimensional results for motions in the in-line direction of two degrees-of-freedom VIV on cylinders with small mass ratio ($m^* \leq 3.0$)

different; therefore, indirectly confirming that the Strouhal number decreases with the aspect ratio decrease. Detailed discussion about this effect can be found, for example, in Fox and Apelt [31] and Stappenbelt and O'Neill [32].

Figure 11 makes a comparison between results for $2.3 < m^* < 2.8$. The results from the literature are from a cantilevered beam tested by Pesce and Fujarra [13] and from an elastically mounted rigid cylinder investigated by Jauvtis and Williamson [14], Stappenbelt and Lalji [16], and Blevins and Coughran [17], as well as from a pivoted pendulum cylinder tested by Freire and Meneghini [18].

Except for the results obtained in the present work, which consider $L/D = 2.0$, all the other results resemble classical ones with upper and lower branches inside the synchronization region. Aside from that and surprisingly, the results from $L/D = 2.0$ have shown nondimensional amplitudes comparable to those for bare cylinders with higher aspect ratio, which deserves a further investigation, particularly related to the fluid dynamic mechanism of the vortex shedding responsible for such a high amplitude response. In fact, Morse et al. [33] discussed a similar behavior by comparing elastically mounted cylinders with $L/D = 8.00$, subjected or not to the free end effects.

For the same case $2.3 < m^* < 2.8$, the in-line results presented in Fig. 12 show a peak amplitude of $A_x/(\gamma D) \cong 0.35$ with a more pronounced dispersion. Again, one can notice a lower branch in the results from Jauvtis and Williamson [14] and Freire and Meneghini [18] with high aspect ratio cylinders, but not the same behavior for the low aspect ratio results.

Finally, Fig. 13 compares the transverse frequencies of oscillation normalized by the transverse natural frequency in still water, all the results for $2.3 < m^* < 2.8$. According to the results from Jauvtis and Williamson [14], the lower branch is characterized by a nearly constant $f_y/f_o \approx 1.05$, behavior not observed for the

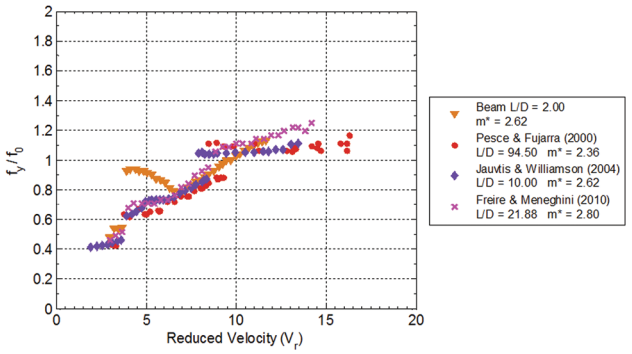

Fig. 13 Comparison between nondimensional results of transverse oscillation frequency and transverse natural frequency in still water for two degrees-of-freedom VIV on cylinders with small mass ratio ($m^* \leq 3.0$)

present results where the ratio f_y/f_o increases in a nearly linear manner, which seems to indicate that the transverse frequencies of oscillation for very short cylinders does not correspond to either the transverse natural frequency nor the shedding frequency for a fixed cylinder. Therefore, one more reason to deeply investigate the two degrees-of-freedom VIV on cylinders with low aspect ratio and $m^* = 1$.

5 General Conclusions

The main purpose was to investigate the VIV on short cylinders and the VIM on floating units drawing a connection between them. Aiming at that, results from experiments with low aspect ratio cylinders presenting small mass ratio were carried out and then compared to those from the literature, focusing on the amplitudes and frequencies of oscillation.

In terms of the transverse amplitudes of response, when comparing the results for different aspect ratios, the higher aspect ratios lead to higher amplitude responses. Also, a small shift in the curves to the right was observed, which can be attributed to possible changes in the Strouhal number for different aspect ratios. Regarding the in-line amplitudes, the results have shown the existence of a later synchronization for the cylinders with lower aspect ratio, consistently with the transverse results.

In terms of frequencies, when coupling between transverse and in-line motions are observed, large amplitudes have occurred. However, an important difference between low and high aspect ratio results is a shift in the synchronization region. For the lower aspect ratio, there is neither an indication of a lower branch nor a close end for the synchronization. Similar behavior was identified by Morse et al. [33] and related to the vortex shedding from the free end of the cylinder.

Finally, even considering results from different apparatuses, namely platforms in small-scale and bare cylinders, the results are quite similar in trend and values, showing that laboratory experiments may well be used in practical investigation, including those concerning the VIM phenomenon acting on platforms.

Acknowledgment

The authors gratefully acknowledge Professor Celso P. Pesce for his support during the discussions of the present work. Also, the authors would like to acknowledge FAPESP and CAPES for the financial support. Professor André L. C. Fujarra is grateful for the support provided by the Brazilian Navy and the Maritime Research Institute Netherlands during his sabbatical year, when the present work was completed.

Nomenclature

γ_n or γ = modal form factor
ρ = water density

ζ_e = structural damping
$A_x/(\gamma D)$ = characteristic nondimensional motion amplitude in the in-line direction
$A_y/(\gamma D)$ = characteristic nondimensional motion amplitude in the transverse direction
D = characteristic diameter
f_o = natural frequency in still water, both in in-line and transverse directions
f_x = oscillation frequency in the in-line direction
f_y = oscillation frequency in the transverse direction
L = immersed length
m = mass per unit length
m_s = oscillating structural mass per unit length
$m^* = 4m_s/\rho\pi D^2$ = mass ratio
L/D = aspect ratio
U = flow velocity
$V_r = U/(f_o.D)$ = reduced velocity considering the natural frequency in still water

References

[1] van Dijk, R. R., Magee, A., Perryman, S., and Gebara, J., 2003, "Model Test Experience on Vortex Induced Vibrations of Truss Spars," Proceedings of the Offshore Technology Conferece (OTC 2003), Houston, Texas, OTC2003-15242.

[2] Finn, L. D., Maher, J. V., and Gupta, H., 2003, "The Cell Spar and Vortex Induced Vibrations," Proceedings of the Offshore Technology Conference (OTC 2003), Houston, Texas, OTC2003-15244.

[3] Irani, M., and Finn, L., 2004, "Model Testing for Vortex Induced Motions of Spar Platforms," Proceedings of the 23rd International Conference on Offshore Mechanics and Arctic Engineering, Vancouver, British Columbia, Canada, OMAE2004-51315.

[4] Finnigan, T., Irani, M., and van Dijk, R. R., 2005, "Truss Spar VIM in Waves and Currents," Proceedings of the 24th International Conference on Offshore Mechanics and Artic Engineering, Halkidiki, Greece OMAE2005-67054.

[5] Roddier, D., Finnigan, T., and Liapis, S., 2009, "Influence of the Reynolds Number on Spar Vortex Induced Motions (VIM): Multiple Scale Model Test Comparisons," Proceedings of the 28th International Conference on Ocean, Offshore and Arctic Engineering. Honolulu, Hawaii, OMAE2009-79991.

[6] Wang, Y., Yang, J., Peng, T., and Li, X., 2009, "Model Test Study on Vortex-Induced Motions of a Floating Cylinder," Proceedings of the 28th International Conference on Ocean, Offshore and Arctic Engineering, Honolulu, Hawaii, OMAE2009-79134.

[7] Gonçalves, R. T., Rosetti, G. F., Fujarra, A. L. C., and Nishimoto, K., 2012, "An Overview of Relevant Aspects on VIM of Spar and Monocolumn Platforms," J. Offshore Mech. Arct. Eng., **134**(1), pp. 0145011–0145017.

[8] Cueva, M., Fujarra, A. L. C., Nishimoto, K., Quadrante, L., and Costa, A., 2006, "Vortex Induced Motion: Model Testing of a Monocolumn Floater," Proceedings of the 25th International Conference on Offshore Mechanics and Artic Engineering, Hamburg, Germany, OMAE2006-92167.

[9] Fujarra, A. L. C., Pesce, C. P., Nishimoto, K., Cueva, M., and Faria, F., 2007, "Non-Stationary VIM of Two Mono-Column Oil Production Platforms," Fifth Conference on Bluff Body Wakes and Vortex-Induced Vibrations, BBVIV5, Costa do Sauipe, Bahia, Brazil.

[10] Gonçalves, R. T., Rosetti, G., Fujarra, A. L. C., and Nishimoto, K., 2012, "Experimental Comparative Study on Vortex-Induced Motion (VIM) of a Monocolumn Platform," J. Offshore Mech. Arct. Eng., **134**(1), pp. 0113011–01130115.

[11] Gonçalves, R. T., Fujarra, A. L. C., Rosetti, G. F., and Nishimoto, K., 2010, "Mitigation of Vortex-Induced Motion (VIM) on a Monocolumn Platform: Forces and Movements," J. Offshore Mech. Arct. Eng., **132**(4), pp. 0411021–04110216.

[12] Gonçalves, R. T., Franzini, G. R., Fujarra, A. L. C., and Meneghini, J. R., 2010, "Two Degrees-of-Freedom Vortex-Induced Vibration of a Circular Cylinder With Low Aspect Ratio," Symposium on Bluff Body Wakes and Vortex-Induced Vibrations, BBVIV6, Capri Island, Italy.

[13] Pesce, C. P., and Fujarra, A. L. C., 2000, "Vortex-Induced Vibrations and Jump Phenomenon: Experiments With a Clamped Flexible Cylinder in Water," Int. J. Offshore Polar Eng., **10**, pp. 26–33.

[14] Jauvtis, N., and Williamson, C. H. K., 2004, "The Effect of Two Degrees of Freedom on Vortex-Induced Vibration at Low Mass and Damping, J. Fluid Mech., **509**, pp. 23–62.

[15] Sanchis, A., Saelevik, G., and Grue, J., 2008, "Two-Degree-of-Freedom Vortex-Induced Vibrations of a Spring-Mounted Rigid Cylinder With Low Aspect Ratio," J. Fluids Struct., **24**, pp. 907–919.

[16] Stappenbelt, B., and Lalji, F., 2008, "Vortex-Induced Vibration Super-Upper Response Branch Boundaries," Int. J. Offshore Polar Eng., **18**, pp. 99–105.

[17] Blevins, R. D., and Coughran, C. S., 2009, "Experimental Investigation of Vortex-Induced Vibration in One and Two Dimensions With Variable Mass, Damping, and Reynolds Number," J. Fluids Eng., **131**(10), pp. 1012021–1012027.

[18] Freire, C. M., and Meneghini, J. R., 2010, "Experimental Investigation of VIV on a Circular Cylinder Mounted on an Articulated Elastic Base With Two Degrees-of-Freedom," Symposium on Bluff Body Wakes and Vortex-Induced Vibrations, BBVIV6, Capri Island, Italy.

[19] Fujarra, A. L. C., Pesce, C. P., Flemming, F., and Williamson, C. H. K., 2001, "Vortex-Induced Vibration of a Flexible Cantilever," J. Fluids Struct., **15**, pp. 651–658.

[20] Jauvtis, N., and Williamson, C. H. K., 2003, "Vortex-Induced Vibration of a Cylinder With Two Degrees of Freedom," J. Fluids Struct., **17**, pp. 1035–1042.

[21] Flemming, F., and Williamson, C. H. K., 2005, "Vortex-Induced Vibrations of a Pivoted Cylinder," J. Fluid Mech., **522**, pp. 215–252.

[22] Dahl, J. M., Hover, F. S., and Triantafyllou, M. S., 2006, "Two-Degree-of-Freedom Vortex-Induced Vibrations Using a Force Assisted Apparatus," J. Fluids Struct., **22**, pp. 807–818.

[23] Leong, C. M., and Wei, T., 2008, "Two-Degree-of-Freedom Vortex-Induced Vibration of a Pivoted Cylinder Below Critical Mass Ratio," Proc. R. Soc. A, **464**, pp. 2907–2927.

[24] Marzouk, O. A., 2010, "Characteristics of the Flow-Induced Vibration and Forces With 1- and 2-DOF Vibrations and Limiting Solid-to-Fluid Density Ratios," J. Vibr. Acoust., **132**(**4**), pp. 0410131–0410139.

[25] Franzini, G. R., Gonçalves, R. T., Fujarra, A. L. C., and Meneghini, J. R., 2010, "Experiments of Vortex-Induced Vibration on Rigid and Inclined Cylinders in Two Degrees of Freedom," Symposium on Bluff Body Wakes and Vortex-Induced Vibrations, BBVIV6, Capri Island, Italy.

[26] Freire, C. M., Korkischko, I., and Meneguini, J. R., 2009, "Development of an Elastic Base With Two Degrees of Freedom for VIV Studies," Proceedings of 20th International Congress of Mechanical Engineering, COBEM 2009, Gramado, RS, Brazil.

[27] Assi, G. R., Meneghini, J. R., Aranha, J. A., Bearman, W., and Casaprima, E., 2006, "Experimental Investigation of Flow-Induced Vibration Interference Between Two Circular Cylinders," J. Fluids Struct., **22**, pp. 819–827.

[28] Blevins, R. D., 1990, *Flow-Induced Vibration*, Krieger, Malabar, FL, p. 72.

[29] Gonçalves, R. T., Franzini, G. R., Rosetti, G., Fujarra, A. L. C., and Nishimoto, K., 2012, "Analysis Methodology for Vortex-Induced Motion (VIM) of a Monocolumn Platform Applying the Hilbert-Huang Transform Method," J. Offshore Mech. Arct. Eng., **134**(1), pp. 0111031–0111037.

[30] Huang, N. E., Shen, Z., Long, S. R., Wu, M. C., Shin, H. H., Zheng, Q., Yen, N. C., Tung, C. C., and Liu, H. H., 1998, "The Empirical Mode Decomposition and the Hilbert Spectrum for Nonlinear and Non-Stationary Time Series Analysis, Proc. R. Soc. London, Ser. A, **454**, pp. 903–995.

[31] Fox, T. A., and Apelt, C. J., 1993, "Fluid-Induced Loading of Cantilevered Circular Cylinders in a Low-Turbulence Uniform Flow. Part 3: Fluctuating Loads With Aspect Ratios 4 to 25," J. Fluids Struct., **7**, pp. 375–386.

[32] Stappenbelt, B., and O'Neill, L., 2007, "Vortex-Induced Vibration of Cylindrical Structures With Low Mass Ratio," Proceedings of the 17th International Offshore and Polar Engineering Conference, Lisbon, Portugal.

[33] Morse, T. L., Govardhan, R. N., and Williamson, C. H. K., 2008, "The Effect of End Conditions on Vortex-Induced Vibration of Cylinders," J. Fluids Struct., **24**, pp. 1227–1239.